XMM-Newton Calibration Technical Note

Status of the EPIC-pn absolute timing capabilities using the Crab pulsar

S. Rosen

December 17, 2024

1 Introduction

This document summarizes the current status of the XMM-Newton EPIC-pn absolute timing capabilities. It is generally updated whenever new calibration observations of the Crab are processed.

2 Calibration observations of the Crab

The Crab pulsar is observed twice yearly with EPIC-pn in both Timing (TI) and Burst (BU) modes as part of the routine observations to calibrate the XMM-Newton relative and absolute timing capabilities. These observations are typically performed ∼6 months apart around February-March, and August-September. Additionally, the Crab has been subject to a number of non-routine calibration observations in both modes. All of these observations are used for the monitoring of the timing capabilities of the EPIC-pn camera. The previous update was reported in CAL-TN-0220.pdf (issue 2.1.0).

The latest observations from XMM-Newton revolution 4531 (2024 Sep 04) have been processed using the most up-to-date public version of SAS (currently SAS v21.0) using the DE200 solar system ephemeris (for consistency with the Jodrell Bank radio ephemeris) and analysed as described in:

`http://xmmweb.esac.esa.int/docs/documents/CAL-TN-0211-1-1.pdf`.

3 Current status of the absolute timing capabilities of EPIC-pn

The absolute timing performance of EPIC-pn is calculated by measuring the delay between the X-ray and the radio pulse. The radio ephemeris is provided by the Jodrell Bank radio telescope, which

Table 1: Absolute timing accuracy of EPIC-pn.

Mode	Pulse delay (μs)
Timing	-306 ± 98
Burst	-368 ± 79
Total	-341 ± 93

observes the Crab regularly ([1]) (see also [1]). We show, in Fig. 1, the pulse delays over the lifetime of the mission. The mean pulse delay values for TI and BU modes, as well as the total, are also reported in Table 1. The 1σ confidence interval (the standard deviation (SD) of the distribution of offsets) can be used as a proxy for the absolute timing accuracy of EPIC-pn. The individual X-ray - radio offsets are shown in table 2. Some measurements are excluded from the final analysis, as described in section 3.1, along with a set of 8 cases with implausibly large offsets, i.e. outside the range (0 > offset > -800 μs) and generally having offsets offsets of $\geq$ 1000μs (1ms) from the mean offset.

3.1 Comments on the current results

The most recent Crab observations, from revolution 4531, included in this update, yield pulse delays relative to the radio ephemeris that are entirely consistent with the distribution of previous delay values.

It should be noted that the Burst mode observations, 0811022801 and 0811022901, from revolution 3436 and 0611182501 from revolution 2713, which show substantially larger negative deviations with respect to the radio ephemeris than the majority of measurements, were made with the source observed directly (source positioned at X,Y = 170,33 in CCD4) rather than in the usual offset position (X,Y=191,38) - the source location in pn CCD4 is given for all observations in table 2. This incurrs a much higher count rate (causing a number of transitions to counting mode) but, more importantly, it is suspected that this positioning may result in incorrect fine-time corrections of perhaps 430 microseconds. We have been conservative and excluded these data from the latest analysis. The Burst mode observation, 0811024301, from rev 3978, which also has a large negative offset with respect to the radio ephemeris, contains a gap of 245s, around 23% of the way into the observation, which is too long to verify potential time jumps. Separate analyses of the timeseries before and after the gap, however, did not yield notably different offsets, though the pre-gap segment, which should be free of time jumps, has a short exposure of only 1800s. In this analysis we also conservatively excluded this observation.

The impact of excluding these observations is to reduce the mean offset of XMM-radio measurements and their scatter, for the Burst mode data alone from -384±101μs to -368±79μs, and for the combined Burst and Timing mode data, from -352±107μs to -341±93μs, respectively.

It is also noted, however, that the Burst and Timing mode data from revolution 3435, where the source is observed in the normal, offset position, show similarly large negative offsets to those from

[1] http://www.jb.man.ac.uk/ pulsar/crab.html

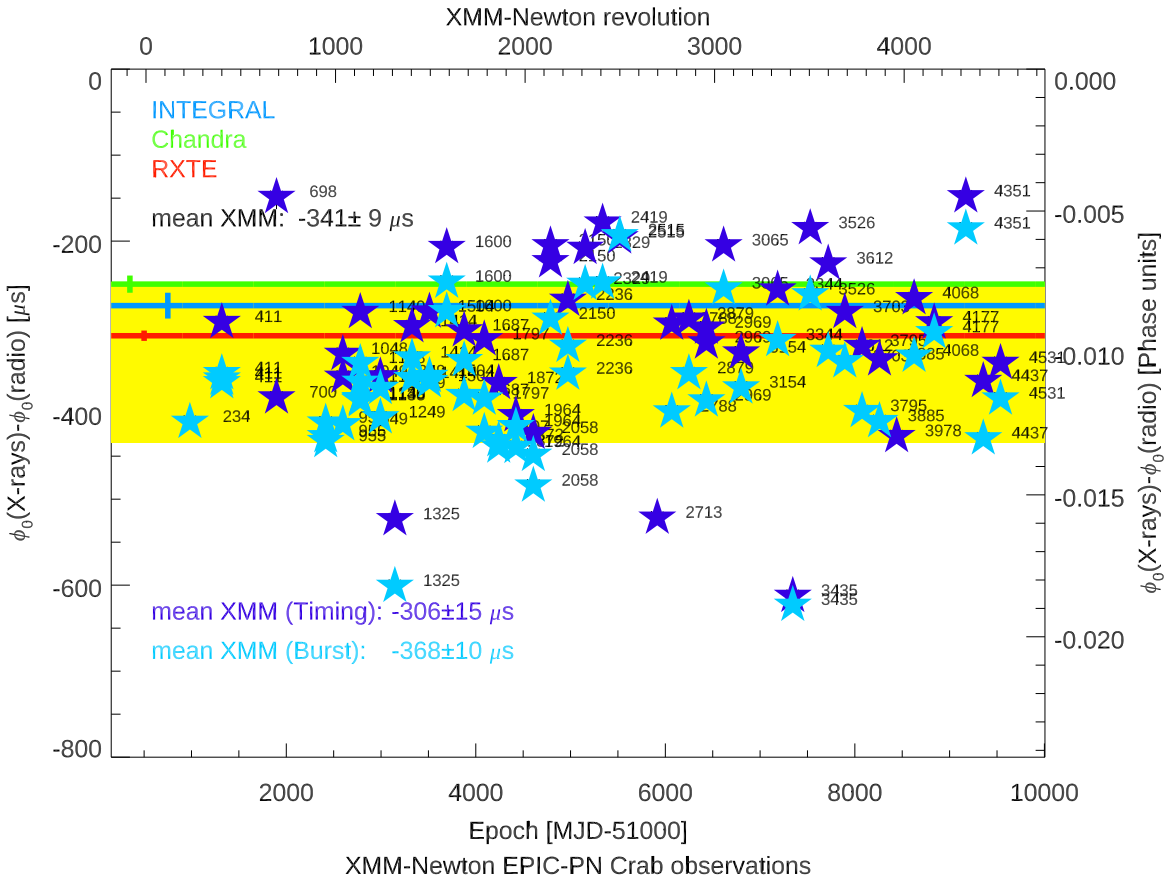

Figure 1: Absolute timing delay measurements of the primary pulses of the Crab pulsar, obtained with the XMM-Newton pn, measured with respect to the Jodrell Bank radio ephemeris. The yellow band indicates the confidence interval of the XMM-Newton measurements in units of $\pm 1\sigma$ (SD) from the mean. The blue, red and green horizontal lines indicate the INTEGRAL, RXTE (Molkov, Jourdain & Roques, 2010, ApJ, 708, 403) and Chandra (see https://cxc.harvard.edu/ccr/proceedings/03_proc/presentations/rots/) measurements, respectively - the small coloured vertical bars in each case indicate their 1σ statistical error. The errors given for the XMM TI, BU and mean XMM offset values, are the formal errors on the mean. It should be noted that the Burst mode observations, 0811022801 and 0811022901, from revolution 3436, 0611182501 from revolution 2713, and 0811024301 from rev 3978, were excluded from the latest analysis.

revolution 3436, where the Crab was observed directly. The Burst and Timing data from revolution 1325 also show large negative offsets but contain no obvious observational problems. These data are retained in the latest analysis. Conversely, some observations in revolutions 1138 and 2969 have the source displaced from the nominal position but yield offsets with respect to the radio that are within the 1σ spread of the ensemble of all measurements.

Table 2: Position of the Crab pulsar (in pixels) on the pn detector (CCD4). Mode is indicated as B(Burst) or T(Timing). The last column contains the time offsets of the pn pulses relative to the radio (X-ray - radio).

Revolution	ObsID	ExposureID	X	Y	Mode	radio offset (μs)
40	0118700201	U002	36	190	B	-8283.42
56	0122330801	U002	37	190	T	-6226.63
234	0135730701	S002	37	190	B	-410.15
411	0153750201	U002	37	190	B	-364.07
411	0153750301	S001	37	190	B	-359.84
411	0153750401	S001	37	190	T	-294.07
411	0153750501	S001	37	190	B	-353.54
698	0160960201	S001	38	190	T	-148.69
700	0160960301	S001	38	191	T	-381.74
874	0160960401	U002	34	170	B	523.14
874	0160960601	U002	33	170	B	8755.17
955	0160960701	S001	38	190	B	-411.06
955	0160960801	S001	37	190	B	-426.88
955	0160960901	S001	37	190	B	-432.51
1048	0160961001	S001	38	190	T	-331.18
1049	0160961101	S001	38	190	B	-412.89
1049	0160961201	S001	38	190	T	-357.74
1140	0160961301	S001	37	191	B	-363.64
1140	0160961401	S001	37	190	T	-282.45
1140	0160961501	S001	37	190	B	-383.65
1138	0312790201	U002	37	140	B	-384.99
1138	0312790401	U002	38	90	B	-382.63
1249	0412590101	S001	38	190	B	-370.77
1249	0412590201	S001	38	191	T	-357.25
1249	0412590301	S001	38	191	B	-404.92
1325	0412590601	S001	37	191	T	-523.36
1325	0412590701	S001	37	190	B	-600.86
1414	0412591001	S001	38	191	B	-335.28
1414	0412591101	S001	38	191	T	-298.97
1414	0412591201	S001	38	191	B	-359.19
1504	0412591401	S001	37	190	B	-356.79
1504	0412591501	S001	37	190	T	-281.94
1504	0412591601	S001	37	190	B	-362.77
1600	0412591901	S001	38	191	B	-281.47
1600	0412592001	S001	38	191	T	-206.93
1600	0412592101	S001	38	191	B	-247.18

Table 2 – Coninued

Revolution	ObsID	ExposureID	X	Y	Mode	radio offset (μs)
1687	0412592401	S001	37	190	B	-379.00
1687	0412592501	S001	37	190	T	-303.84
1687	0412592601	S001	37	190	B	-338.42
1797	0412593001	S001	37	191	B	-383.08
1797	0412593101	S001	37	190	T	-314.16
1797	0412593201	S001	37	190	B	-421.76
1872	0611180101	S003	37	190	B	-438.86
1872	0611180201	S003	37	190	T	-365.10
1872	0611180301	S003	37	190	B	-431.49
1964	0611180401	S003	38	191	B	-415.15
1964	0611180501	S003	38	191	T	-402.47
1964	0611180601	S003	38	191	B	-439.30
2058	0611180701	S003	37	191	B	-448.55
2058	0611180801	S003	37	191	T	-423.07
2058	0611180901	S003	37	191	B	-484.25
2150	0611181001	S003	38	191	T	-223.44
2150	0611181101	S003	38	190	T	-204.93
2150	0611181201	S003	38	191	B	-290.25
2236	0611181301	S003	37	190	B	-354.09
2236	0611181401	S003	37	190	T	-268.27
2236	0611181501	S003	37	191	B	-321.80
2329	0611181601	S003	38	190	T	-207.90
2329	0611181701	S003	38	191	B	-249.72
2419	0611181801	S003	37	190	T	-178.47
2419	0611181901	S003	37	190	B	-248.18
2515	0611182001	S003	38	191	T	-195.68
2515	0611182101	S003	38	191	B	-193.19
2607	0611182201	S003	37	191	T	12143.83
2607	0611182301	S003	37	191	B	-2449.79
2713	0611182401	S003	37	191	T	-521.60
2788	0611182601	S003	37	190	T	-296.00
2788	0611182701	S003	37	190	B	-398.09
2879	0611182801	S003	38	191	T	-290.23
2879	0611182901	S003	38	191	B	-353.56
2969	0611183001	S003	28	11	T	-317.80
2969	0611183101	U002	38	191	B	-385.27
2969	0611183201	S003	37	190	T	-300.64
3065	0611183301	S003	38	191	B	-255.03
3065	0611183401	S003	38	191	T	-204.98
3154	0793980101	S003	37	190	B	-370.20
3154	0793980201	S003	37	190	T	-329.54
3261	0793980301	S003	37	191	B	-1438.39
3261	0793980401	S003	37	191	T	-1375.06
3344	0811022401	S001	37	190	T	-256.24
3344	0811022501	S001	37	190	B	-314.99
3435	0811022601	S001	38	191	T	-612.50

Table 2 – Coninued

Revolution	ObsID	ExposureID	X	Y	Mode	radio offset (μs)
3435	0811022701	S001	37	191	B	-622.92
3526	0811023001	S001	37	190	T	-184.94
3526	0811023101	S001	37	190	B	-261.91
3612	0811023201	S001	37	190	T	-226.03
3612	0811023301	S001	38	190	B	-327.64
3703	0811023501	S001	37	191	T	-282.47
3703	0811023601	S001	37	190	B	-339.72
3795	0811023701	S001	38	190	T	-321.92
3795	0811023801	S001	38	191	B	-397.60
3885	0811024001	S001	37	190	T	-337.50
3885	0811024101	S001	37	190	B	-409.25
3978	0811024201	S001	38	190	T	-426.72
4068	0811024501	S001	37	190	T	-266.39
4068	0811024601	S001	37	190	B	-333.25
4177	0811025101	S001	37	191	T	-294.47
4177	0811025301	S001	38	190	B	-305.95
4351	0811025701	S001	38	191	T	-147.92
4351	0811025801	S001	38	190	B	-185.30
4437	0811025901	U002	37	190	T	-362.64
4437	0811026001	S001	37	190	B	-429.31
4531	0811026101	U002	38	191	T	-341.66
4531	0811026201	S001	38	191	B	-383.03

4 References

References

[1] Lyne, A. G., Pritchard, R. S. & Graham-Smith, F. 1993. MNRAS, 265, 1003